



## Article

# Soil Potassium Balance in the Hilly Region of Central Sichuan, China, Based on Crop Distribution

Shan Wang <sup>1</sup>, Zhiping Li <sup>2</sup>, Lulu Li <sup>2</sup>, Yuelin Xu <sup>2</sup>, Guohui Wu <sup>2</sup>, Qin Liu <sup>3</sup>, Peihao Peng <sup>1,\*</sup> and Ting Li <sup>2,\*</sup>

<sup>1</sup> College of Earth Sciences, Chengdu University of Technology, Chengdu 610059, China; 2019010042@stu.cduto.edu.cn

<sup>2</sup> College of Resources, Sichuan Agricultural University, Chengdu 611130, China; lzhiping2023@163.com (Z.L.)

<sup>3</sup> Institute of Mountain Hazards and Environment, Chinese Academy of Sciences, Chengdu 610041, China

\* Correspondence: pengpeihao@cdut.edu.cn (P.P.); tingli121@sicau.edu.cn (T.L.)

**Abstract:** The problem of soil fertility imbalance in hilly agriculture is prominent, and accurate estimation of soil potassium balance is key to achieving precision fertilization at the regional level. Crop distribution has a significant impact on potassium balance, but studies on potassium balance with a focus on crop cultivation types are scarce, especially with regard to hilly areas. In this study, the spatial distribution characteristics of soil potassium balance under different cropping conditions and its influencing factors were analyzed for a hilly region. The results showed that (1) the soil rapidly available potassium (RAK) and slowly available potassium (SAK) content in the 0–20 cm soil layer ranged from 29.37 to 122.07 mg kg<sup>-1</sup> and from 472.31 to 772.77 mg kg<sup>-1</sup>, respectively. (2) The soil potassium equilibrium status varied considerably among different cropping systems and the soil potassium deficit was greatest under the rapeseed–maize rotation, reaching -129.50 kg K ha<sup>-1</sup> yr<sup>-1</sup>. The difference in soil potassium deficits between the rice–rapeseed and wheat–maize rotations was not significant, at -46.79 kg K ha<sup>-1</sup> yr<sup>-1</sup> and -44.07 kg K ha<sup>-1</sup> yr<sup>-1</sup>, respectively, and only the rice–wheat rotation showed a potassium surplus. Due to the low potassium absorption of crops, the equilibrium value of soil potassium is higher than that of crop rotation, and rice and wheat can achieve different degrees of potassium surplus. Rapeseed planting was generally under-applied with potassium, and the potassium deficit could reach -70 kg K ha<sup>-1</sup> yr<sup>-1</sup>. (3) Climate, topography, anthropogenic activity, and soil available potassium explained 20.8% of the variance in soil potassium balance. Anthropogenic activity such as roads and population density had the greatest influence, with 0.797. Topography and average annual precipitation had the weakest influences. These findings emphasize the importance of anthropogenic activity for soil potassium balance, and also provide regional evidence for formulating efficient measures for regional potassium resources management.



**Citation:** Wang, S.; Li, Z.; Li, L.; Xu, Y.; Wu, G.; Liu, Q.; Peng, P.; Li, T. Soil Potassium Balance in the Hilly Region of Central Sichuan, China, Based on Crop Distribution. *Sustainability* **2023**, *15*, 15348. <https://doi.org/10.3390/su152115348>

Academic Editor: Teodor Rusu

Received: 18 August 2023

Revised: 21 October 2023

Accepted: 24 October 2023

Published: 27 October 2023



**Copyright:** © 2023 by the authors. Licensee MDPI, Basel, Switzerland. This article is an open access article distributed under the terms and conditions of the Creative Commons Attribution (CC BY) license (<https://creativecommons.org/licenses/by/4.0/>).

## 1. Introduction

Hilly landscapes, as one of the five major terrestrial geomorphological types globally, play a critical role in agricultural production. Soil nutrient management in hilly areas becomes particularly crucial because hilly agriculture is susceptible to soil fertility imbalances. Exploring the characteristics of fertility balance and its influencing mechanisms is important for scientific management of hilly agriculture. Potassium (K) plays an important role in plant growth, and its deficiency or absence has a significant impact on normal plant growth and development, cellular metabolism, and resistance to insect pests [1,2]. Although potassium is one of the most abundant nutrients in soil, soil potassium distribution shows strong spatial heterogeneity due to the high spatial and temporal variability in soil resources [3–5]. Fertilization is the most direct and effective way to augment and regulate soil potassium content [6–8]. However, differences in nutrient inputs, climatic and soil conditions, different crop assortment, and yield level all affect crop demand for

potassium and its soil outflow, both of which ultimately affect the potassium balance [9]. Therefore, understanding the soil potassium balance in a soil–crop system is a priority when attempting to ensure a stable and high yield of crops and achieve efficient management of potassium resources.

Soil potassium balance is a measure of the sum of potassium inflows and outflows within a particular framework [10,11]. Currently, there are two main types of research on potassium balance in farmland soil both domestically and internationally: soil potassium balance based on crop soil fertilization experiments, and soil potassium balance estimation based on statistical or survey data. For instance, based on a field study, Li et al. [12] demonstrated that zeolite amendments alleviated negative potassium balances, and Zhang et al. [13] found that high straw return with fertilization improved soil potassium supply and potassium balance, compared to no fertilization or low straw return conditions. These studies provide practical ways to improve potassium balance, but do not reveal the statuses of regional potassium balances. In contrast, Linquist et al. [14] assessed soil potassium balance (average value was  $-15 \text{ kg K ha}^{-1} \text{ yr}^{-1}$ ) in commercial rice fields across California based on historical information provided by growers, and Liu et al. [15] analyzed temporal and spatial changes in the potassium balance of farmland in China from 1980 to 2015 using statistical data and related parameters. Although previous studies have obtained the total provincial soil potassium balance, which is of some significance in guiding regional fertilization, they did not take into account the spatial variation in soil potassium balance within a region due to crop distribution. Previous research on soil potassium spatial characteristics has mainly focused on spatial variation in soil potassium fertility and analysis of influencing factors [3,4,12], but has paid less attention to the spatial mapping of soil potassium balance in terms of regional crop distribution. However, when assessing the nutrient balance of the farmland in a region, the spatial distribution of regional crops can often better represent the regional farmland’s nutrient balance and shows the regional farmland’s nutrient surplus and deficit situation in a more realistic way.

Therefore, considering the fact that planting structure has an important effect on potassium distribution but few studies have quantified it, especially in hilly areas where soil fertility exchanges are more frequent, this study attempted to explore the spatial distribution characteristics of soil potassium balance under different cropping conditions in a hilly region. Shehong County, Suining City, located in the core hilly area of Sichuan Province, possessing typical hilly agriculture, was selected as the study area. Multi-temporal Sentinel-2 satellite images and the decision-tree classification method were used to extract the spatial distribution of major crops in the study area. The spatial distribution pattern for soil potassium content was also assessed using soil sampling data. The spatial distribution pattern of soil potassium content was evaluated through soil sampling data, and further combined with the spatial distribution of regional crops. Based on a consideration of different forms of soil potassium input and soil potassium output, the potassium balance characteristics of farmland soil in the study area were calculated, and their spatial distribution differences and influencing factors were analyzed, in order to provide references for rational potassium fertilizer application and improving soil potassium utilization efficiency in the region.

## 2. Materials and Methods

### 2.1. Study Area

Due to the diverse planting structure and complex terrain conditions in hilly areas, the management of soil potassium in these areas is often difficult. Therefore, the study of potassium balance in hilly areas is particularly important. This study was conducted in Shehong County, Sichuan Province, China, which is dominated by hilly terrain and lies between  $105^{\circ}10' \text{ E}$ – $105^{\circ}40' \text{ E}$  and  $30^{\circ}37' \text{ N}$ – $31^{\circ}12' \text{ N}$  (Figure 1). The altitude within the territory ranges from 280 m to 664 m, and is high in the northwest and low in the southeast. This area belongs to the subtropical humid climate zone and has a mild climate. The county covers  $1496 \text{ km}^2$  and is a rich agricultural resource. Its total arable land area is  $70,060.87 \text{ hm}^2$ . According to China Soil System Classification (1995), the main soil-forming

parent materials in this region are the Penglai Group soils and three gray-brown alluvium-covered soil types (purplish soils, paddy soils, and alluvial soils), and the main crop types are rice, corn, wheat, and rape.

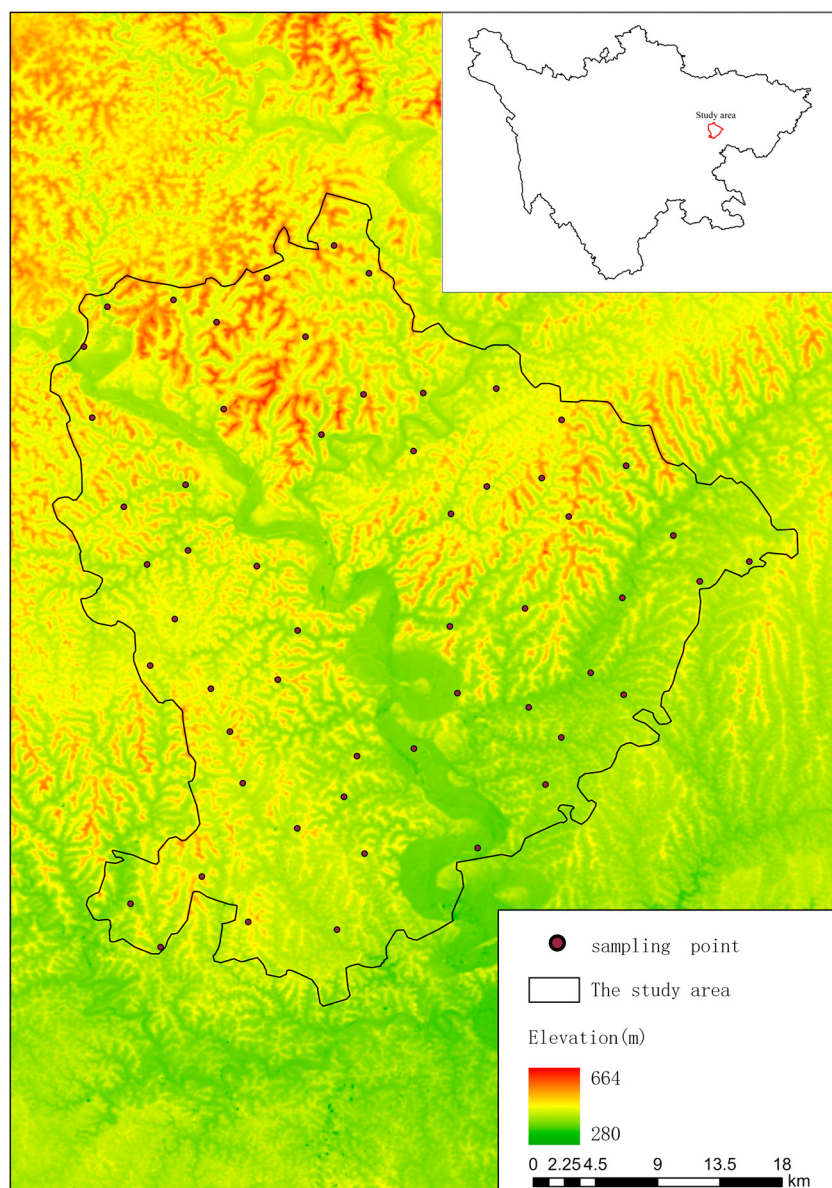


**Figure 1.** The location of the study area in Sichuan Province.

## 2.2. Soil Sample Collection and Laboratory Analysis

Potential sampling points were first identified indoors based on soil type, soil-forming parent material, and topographic factors. Then, based on reachability and the actual state of the sampling sites, 56 sampling points were identified (Figure 2). A global positioning system device was used to measure geographic coordinates and elevation at each location. Crop cultivation and other information for each site was also collected during field investigation. Three soil cores were randomly collected from each site using a standard Edelman auger with a diameter of 7 cm, and each soil sample weighed approximately 1 kg. The samples were air-dried, after thorough homogenization and removal of roots and stone, and finely ground to pass through a sieve with openings smaller than 2 mm. Soil rapidly available potassium (RAK) was leached with  $1.0 \text{ mol L}^{-1}$  neutral  $\text{NH}_4\text{OAC}$  at a 10:1 water-soil ratio and slowly available potassium (SAK) was leached with  $1 \text{ mol L}^{-1}$  boiling  $\text{HNO}_3$  at a 10:1 water-soil ratio. The filtrate of soil sample solution was measured using

the flame photometric method [16]. Soil available potassium (AK) was the summation of RAK and SAK.

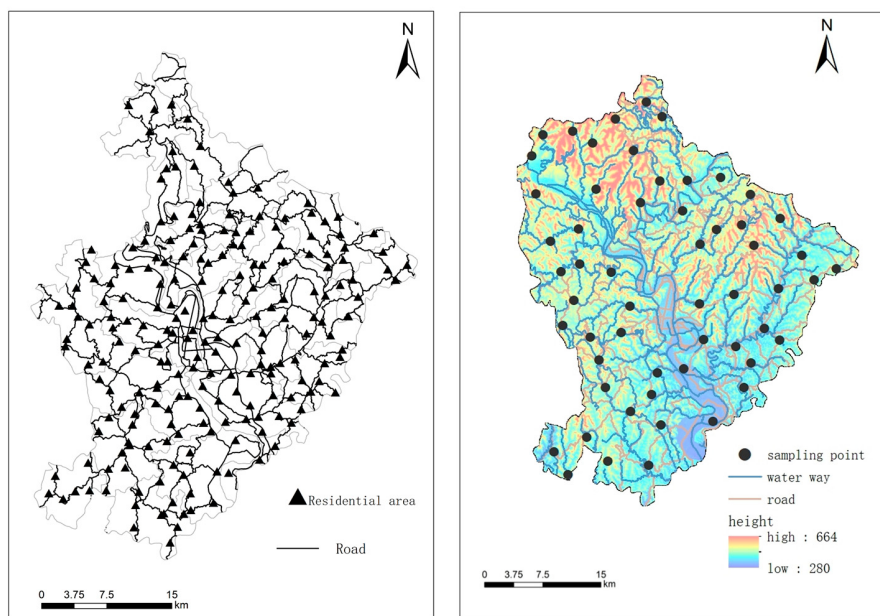


**Figure 2.** Study area: basic geographic information, and location of the soil sampling sites.

### 2.3. Cropping Pattern Extraction

Many sophisticated supervised classification algorithms have been developed to identify crop types with multiple vegetation indices [17]. Among them, the decision tree method is widely used to identify crop planting structure due to its high computational efficiency and strong regional applicability. Therefore, a decision tree classification process was designed to achieve a simple, fast, and accurate extraction of crop patterns (Figure 3). First, the cloud-free Sentinel-2 L1C images from May 2018 to April 2019 were reprocessed using radiometric calibration, atmospheric correction, and resampling. The normalized difference vegetation index (NDVI) and modified chlorophyll absorption ratio index (MCARI), which are based on the phonological differences among rice, maize, wheat, and oilseed rape, were used to classify the croplands. The crop samples were constructed by combining visual interpretations of the images with field investigation. Finally, the decision tree was trained using the selected samples and classification features.

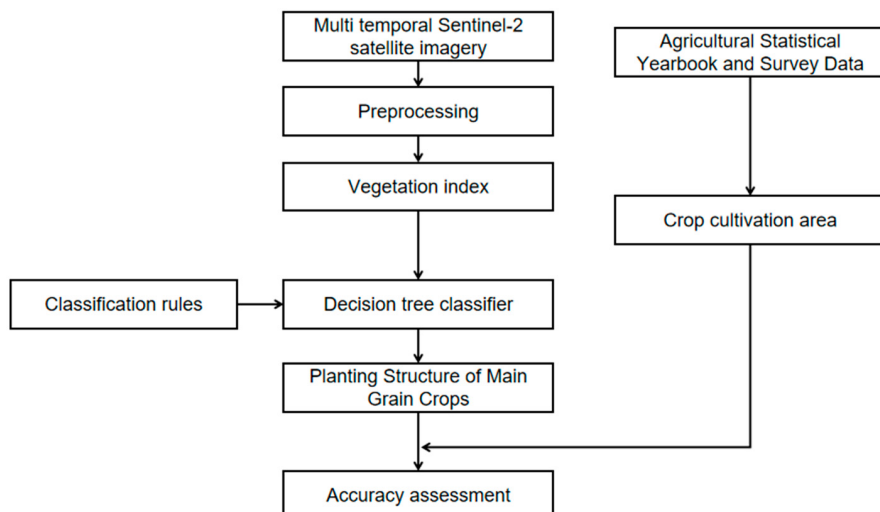


**Figure 3.** Schematic representation of cropping pattern extraction.

#### 2.4. Calculation of On-Farm Potassium Balance

The input of farmland potassium includes: (1) Chemical fertilizer application: the survey data, provided by the County Agricultural Bureau, the Statistics Bureau, visiting farmers, etc. The amount of field fertilizer application collected in this study is the compound fertilizer application amount, which does not include nitrogen fertilizer, phosphorus fertilizer, etc., and has been converted into the input amount of potassium fertilizer ( $K_2O$ ). Due to the organic fertilizer input from livestock and poultry manure and the fertilizer range of the main grain crops in the study area being small, in this study, the input of organic manure from livestock and poultry manure for main grain crops was measured as 0; (2) Potassium amount brought into farmland by rainfall: the average value was obtained via reference literature. The annual averages for potassium in rice–rape, rice–wheat, single-season rice, and the other planting systems were  $15.1 \text{ kg K ha}^{-1} \text{ yr}^{-1}$  [18],  $13.3 \text{ kg K ha}^{-1} \text{ yr}^{-1}$  [18],  $6.5 \text{ kg K ha}^{-1} \text{ yr}^{-1}$  [18], and  $8.3 \text{ kg K ha}^{-1} \text{ yr}^{-1}$  [19], respectively. (3) The amount of potassium deriving from irrigation water. The total potassium input was determined according to the total amount of irrigation water and the potassium content of the irrigation water. The potassium amount in rice–rape, rice–wheat and single-season rice through irrigation water was calculated as  $23.25 \text{ kg K ha}^{-1} \text{ yr}^{-1}$  [18],  $17.6 \text{ kg K ha}^{-1} \text{ yr}^{-1}$  [18],  $17.8 \text{ kg K ha}^{-1} \text{ yr}^{-1}$  [18], respectively, and  $14.8 \text{ kg K ha}^{-1} \text{ yr}^{-1}$  [19] under other planting systems; (4) Soil potassium deriving from returning crop straw to the field: the rate of returning crop straw to the field in the study area was 48.8% [20] and the potassium nutrient content of the straw was 1.9%, 0.99%, 1.16%, and 2.01% [21] for rice, maize, wheat, and oilseed rape, respectively.

Without considering the loss of fertilizer, the potassium outputs from a farm consist of the amount of leaching and the amount of potassium uptake required for the desired economic yield of the crop. In this study, the loss of soil potassium was mainly caused in paddy fields, so the amount of leaching was considered to be  $10 \text{ kg ha}^{-1} \text{ yr}^{-1}$  [19] and potassium uptake by a crop was calculated using Equation (1):

$$K = \sum_{i=1}^n Y * AK_i / Si \quad (1)$$

where  $K$  is the potassium nutrient content ( $K_2O$ ) per unit area of crop uptake,  $\text{kg hm}^{-2}$ ;  $i$  is the value when the crop is present;  $Y$  is the economic yield for a crop, and  $AK$  is the amount of potassium nutrients required per unit economic yield of various crops. In this study, the amount of potassium nutrients required per unit economic yield of rice, wheat, maize, and rape production were  $26.3 \text{ kg t}^{-1}$ ,  $24.7 \text{ kg t}^{-1}$ ,  $21.6 \text{ kg t}^{-1}$ , and  $58.1 \text{ kg t}^{-1}$ , respectively.  $Si$  is the sown area of each crop, which was obtained from the statistical yearbook.

Soil potassium balance is the difference between soil potassium input and soil potassium output, i.e., soil potassium balance = potassium input – potassium output.

#### 2.5. Spatial Analysis of Potassium Balance Based on Ordinary Kriging

Ordinary kriging is a linear geostationary method that produces a good interpolation when the soil dataset is normally distributed and meets the second-order smooth assumption or quasi-second-order smooth assumption. In this study, a normality test, a global trend test, and a spatial autocorrelation test were performed using ArcGIS10.6 (Esri, Redlands, CA, USA) to remove outliers and trend effects. Ordinary kriging interpolation was then performed for RAK and SAK based on the parameters from the best fitted semi-variance model. The interpolation performance was evaluated using the cross-validation method with normalized root mean square error (NRMSE).

## 2.6. The Relationships between Environmental Factors and Potassium Balance

### 2.6.1. Environmental Factors Acquisition

The climatic data, which consisted of mean annual temperature (MAT) and mean annual precipitation (MAP), were obtained from the National Meteorological Information Center (<http://data.cma.cn/site/index.html>, accessed on 10 June 2020).

The DEM data were derived from ASTER GDEM V2 global digital elevation data downloaded from the Geospatial Data Cloud (<http://www.gscloud.cn/>, accessed on 10 June 2020) with a spatial resolution of 30 m. Two topographic factors, regional slope and terrain relief, were extracted using the ArcGIS spatial analysis module.

The vector data for county-level administrative divisions, roads, and rivers were obtained from the National Geographic Information Resources Catalog Service System (<http://www.webmap.cn/>, accessed on 10 June 2020) and the population density grid data were obtained from the shared service platform of the National Earth System Science Data Center (<http://www.geodata.cn/>, accessed on 10 June 2020).

### 2.6.2. Effects of Environmental Factors on Potassium Balance

Firstly, the area was graded to generate a 500 m × 500 m grid pattern and soil potassium input, potassium output, potassium balance, and crop areas of different crop fields within the grid were determined. The environmental factors, such as MAT, MAP, elevation, slope, topographic relief, average road density, and average population density, were then extracted within the grid. Correlations between the environmental factors and potassium balance were analyzed using SPSS data analysis software (IBM SPSS Statistics19, IBM, Somers, NY, USA). MAT and MAP were categorized as climatic factors. Elevation, slope, and topographic relief were categorized as topographic factors, whereas average road density and average population density were categorized as anthropogenic activity factors. The structural equation model (SEM) was constructed from these potassium balance indicators using AMOS software (IBM PSAS AMOS 21, IBM, Chicago, IL, USA) to predict the interactions between soil potassium balance and environmental factors such as climate, topography, anthropogenic activity, and AK content of the soil.

The SEM used several model fitness parameters to judge the reasonableness of the model. These were chi-square ( $\chi^2$ ), degrees of freedom (df), gradient, root mean square error of approximation (RMSEA), and the goodness-of-fit index (GFI). The chi-square ( $\chi^2$ ) test, degrees of freedom (df), gradient index, root mean square error of approximation (RMSEA), and goodness-of-fit index (GFI) are critical metrics in evaluating a model. Specifically, the chi-square ( $\chi^2$ ) test gauges the divergence between observed and model-predicted data. A significant  $\chi^2$  value indicates that the model does not adequately represent the observed data, necessitating adjustments in model structure or parameters. Degrees of freedom (df) measure the model's complexity by indicating how many parameters can be freely modified. A lower df value relative to sample size suggests a simpler model, thereby reducing the risk of overfitting. Meanwhile, the gradient index helps assess the degree of maximum likelihood optimization in the model; a smaller gradient signifies better optimization, while a larger one suggests the need for further refinement. RMSEA evaluates the model's fit quality, accounting for its complexity, and assesses the closeness between the model-predicted and actual observed covariance matrices. Lower RMSEA values imply a better fit, while higher values suggest the contrary. Lastly, the GFI offers a comprehensive assessment, reflecting how closely the model's predicted covariance matrix aligns with the observed one. A higher GFI score indicates a better model fit. Collectively, these metrics serve as a multi-faceted framework for evaluating structural equation models (SEM), aiding in determining model plausibility, identifying areas for improvement, and verifying the model's accuracy for interactions between environmental factors and soil potassium balance. The formulae of  $\chi^2$ , RMSEA, GFI are as follows [22]:

$$\chi^2 = (N - 1)/f \quad (2)$$

$$RMSEA = \sqrt{\frac{\max(\chi^2 - df, 0)}{df(N - 1)}} \quad (3)$$

$$GFI = \frac{\rho}{\rho + 2 \left( \frac{\chi^2_{\text{df}} - df}{N-1} \right)} \quad (4)$$

In the formulae:  $N$ , sample size;  $f$ , minimized discrepancy function;  $df$ , degrees of freedom;  $\rho$ , number of observed variables. When these parameters satisfied  $\chi^2/df < 3$ , RMSEA < 0.08, and GFI > 0.9, then the model was considered to be reasonably fit.

### 3. Results

### 3.1. Spatial Distribution Characteristics of Cropping Patterns

The spatial distributions of the main four crop types were extracted from the decision tree. The extraction accuracy for rice, maize, rape, and wheat were 89.36%, 87.16%, 87.85%, and 84.65%, respectively, when compared to the Statistical Yearbook. The extraction areas were 9705.22 ha, 16,147.55 ha, 5443.56 ha, and 17,414.04 ha for rice, maize, rape, and wheat, respectively, and the maize and wheat cultivation areas were much greater than those of rice and rape (Figure 4). The distributions of the rice–rape rotation, rice–wheat rotation, rape–maize rotation, and wheat–maize rotation areas were obtained using the spatially overlaid method. The rice–rape rotation, rice–wheat rotation, rape–maize rotation, and wheat–maize rotation areas were 896.76 ha, 1868.92 ha, 833.48 ha, and 2106.52 ha, respectively. Maize and wheat were the main cultivated crops in the study area and they accounted for the largest crop areas in every township.

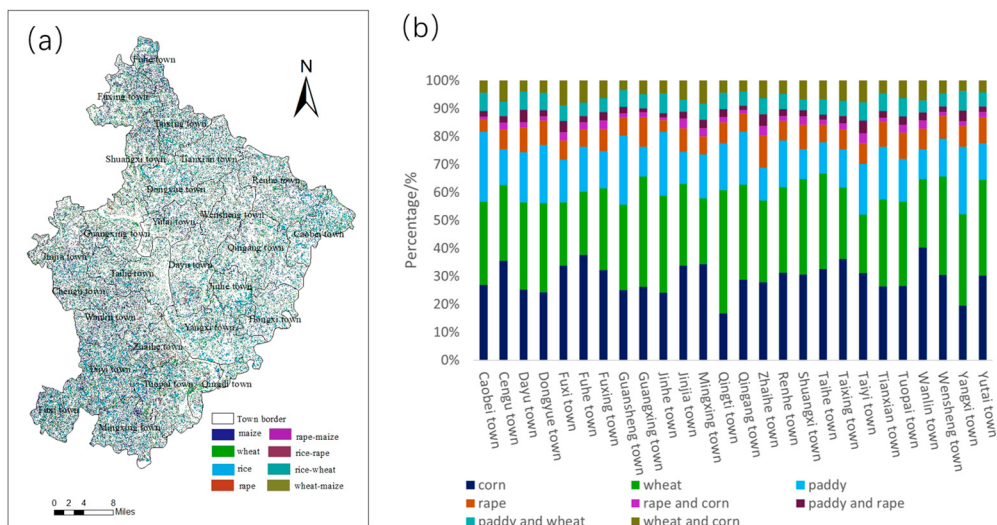


**Figure 4.** Distributions of the different cropping patterns. (a) The cropping patterns map, (b) the proportions of different crop systems in different districts and counties.

### *3.2. Spatial Distribution of Soil Available Potassium*

The spatial distributions of soil RAK and SAK in the study area were determined by kriging interpolation (Figure 5). Kriging performed well in providing reliable estimates of spatial distributions of RAK and SAK, with MSE lower than 0.04 and RMMSE closer to 1. The value of RAK content ranged from 29.37 to 122.07 mg kg<sup>-1</sup>, with an average value of 63.63 mg kg<sup>-1</sup>, and the soil SAK content ranged from 472.31 to 772.77 mg kg<sup>-1</sup>, with an average value of 649.77 mg kg<sup>-1</sup> (Table 1). According to the fertility grading standard of the second national soil census, the soil RAK content in the study area was classified as low level, and the soil SAK was generally at a low or moderate level. The spatial distribution of soil RAK was generally characterized as high in the central townships and low in the north and south townships, similarly to the spatial distribution of soil SAK.

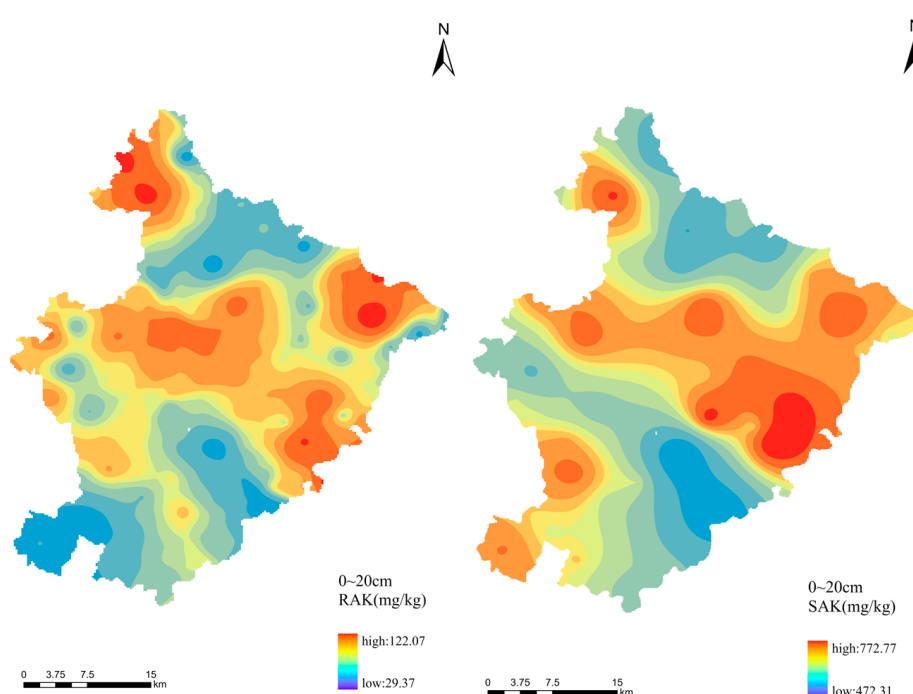


**Figure 5.** Spatial distribution of soil available potassium.

**Table 1.** Geostatistical analysis of RAK and SAK.

Soil Potassium	Min. (mg/kg)	Max. (mg/kg)	Mean (mg/kg)	Standard Deviation (mg/kg)	Nugget Effect (%)	Range (km)	RMMSE	MSE
RAK	29.37	122.07	63.63	11.90	78.18	7.28	1.04	0.04
SAK	472.31	772.77	649.77	46.43	53.72	19.31	0.99	0.01

Note: RAK means rapid available potassium; SAK means slowly available potassium; AVG means average value; MSE means mean standardized error; RMSSE means root mean square standardized error.

The nugget effects of RAK and SAK were greater than 50%, revealing strong spatial variability of soil available potassium, which indicated that anthropogenic activity, such as cropping pattern and field fertilization, had a greater influence than natural environmental factors. The nugget effect of SAK was 53.72%, which was lower than that of RAK, suggesting that SAK was less influenced by anthropogenic activity because its morphology is more stable and it includes the part that could not be directly absorbed and utilized by crops.

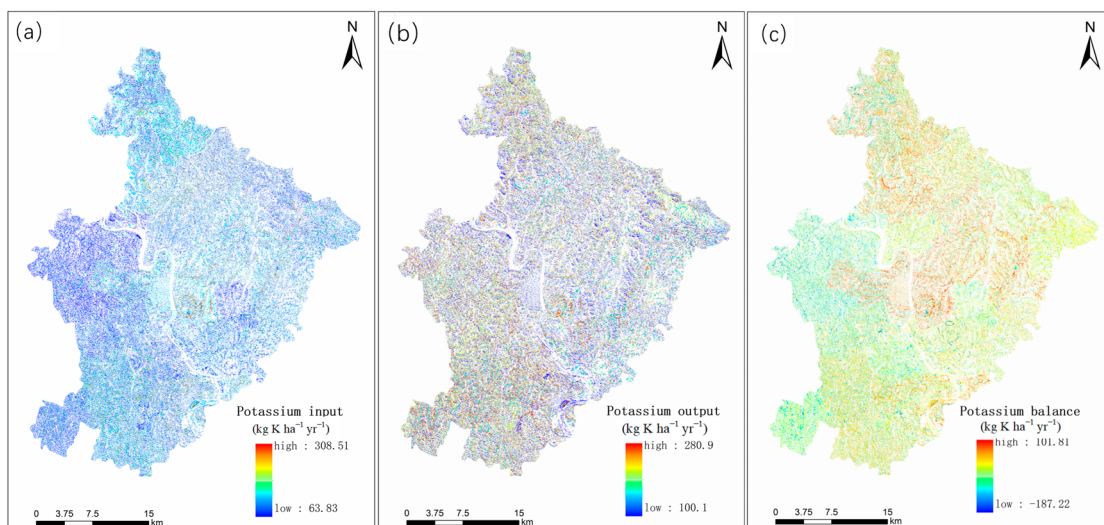
### 3.3. Spatial Distribution of Soil Potassium Balance

The results for the different sources of soil potassium showed that they were significantly different under the various cropping patterns (Table 2). Specifically, under the same cropping pattern, the overall order for potassium input from the different sources was straw return > irrigation water > rainfall input. All three sources of potassium input, i.e., rainfall input, irrigation water, and straw, were highest in the rice–rapeseed rotation, at 15.10, 23.30, and 57.91 kg K ha<sup>-1</sup> yr<sup>-1</sup>, respectively. However, rainfall input was lowest for the rice monoculture (6.50 kg K ha<sup>-1</sup> yr<sup>-1</sup>) and irrigation water was lowest under the maize monoculture, wheat monoculture, rapeseed monoculture, rapeseed–maize rotation, and wheat–maize rotation (14.80 kg K ha<sup>-1</sup> yr<sup>-1</sup>). The potassium input from straw was lowest under the wheat monoculture (13.73 kg K ha<sup>-1</sup> yr<sup>-1</sup>).

**Table 2.** Soil potassium inputs under different cropping patterns ( $\text{kg K ha}^{-1} \text{yr}^{-1}$ ).

Cropping Pattern	Rainfall	Irrigation Water	Straw
Rice monocrop	6.5	17.8	38.88
Maize monocrop	8.3	14.8	15.55
Wheat monocrop	8.3	14.8	13.73
Rape monocrop	8.3	14.8	19.03
Rice–rape rotation	15.1	23.3	57.91
Rice–wheat rotation	13.3	17.6	52.61
Rape–maize rotation	8.3	14.8	34.58
Wheat–maize rotation	8.3	14.8	29.28

The total soil potassium input and the potassium inputs from each township were counted. The results showed that the annual potassium input mostly ranged from 63.83 to 100  $\text{kg K ha}^{-1} \text{yr}^{-1}$  in the study area. There were a few areas where the annual potassium input was greater than 220  $\text{kg K ha}^{-1} \text{yr}^{-1}$  (Figure 6a). The areas with an annual potassium input of less than 100  $\text{kg K ha}^{-1} \text{yr}^{-1}$  were mainly located in the hilly townships at the edge of the study area and the areas  $> 220 \text{ kg K ha}^{-1} \text{yr}^{-1}$  were mainly in the central part of the study area.

**Figure 6.** Spatial distribution maps of potassium input (a), potassium output (b), and potassium balance (c).

The data on potassium uptake by crops were obtained from the literature rather than field measurements and differences between crop varieties were not considered. This meant that cropping pattern was the main reason for the spatial distribution differences in potassium output (Figure 6b). Annual soil potassium output in the study area mostly ranged from 100–204  $\text{kg K ha}^{-1} \text{yr}^{-1}$  and the potassium output of each township ranged from 129.27–144.33  $\text{kg K ha}^{-1} \text{yr}^{-1}$ .

The soil potassium balance for farmland ranged from  $-187.22$  to  $101.81 \text{ kg K ha}^{-1} \text{yr}^{-1}$  and the largest soil potassium deficit was in the southwest of the study area. Soil potassium achieved balance in the northeast and was in surplus in the central part of the study area, with a maximum of  $101.81 \text{ kg K ha}^{-1} \text{yr}^{-1}$  (Figure 6). The soil potassium balance results for the different cropping patterns showed that the rapeseed–maize rotation had the most severe deficit at  $129.50 \text{ kg K ha}^{-1} \text{yr}^{-1}$  (Table 3). The difference in soil potassium deficit between the rice–rapeseed and wheat–maize rotations was not significant, at  $46.79 \text{ kg K ha}^{-1} \text{yr}^{-1}$  and  $44.07 \text{ kg K ha}^{-1} \text{yr}^{-1}$ , respectively. Only the rice–wheat rotation showed a potassium surplus. Low potassium uptake by crops in the monoculture systems meant that the soil potassium balance was higher for the monoculture systems than for the

rotation systems. The oilseed rape areas were generally deficient in potassium by around  $-70.12 \text{ kg K ha}^{-1} \text{ yr}^{-1}$ , which was a higher deficit than those of the rice–rapeseed and wheat–maize rotations.

**Table 3.** Soil potassium balances for each cropping pattern.

Cropping Pattern	K Input		K Output		K Balance	
	Total (t)	Per Hectare ( $\text{kg K yr}^{-1}$ )	Total (t)	Per Hectare ( $\text{kg K yr}^{-1}$ )	Total (t)	Per Hectare ( $\text{kg K yr}^{-1}$ )
Rice monocrop	890.30	137.92	752.66	116.60	137.65	21.32
Maize monocrop	1163.48	88.69	1624.03	123.80	-460.554	-35.11
Wheat monocrop	1580.23	115.74	1366.72	100.10	213.51	15.64
Rapeseed monocrop	306.37	86.98	553.39	157.10	-247.01	-70.12
Rice–rapeseed rotation	255.09	216.90	310.12	263.70	-55.03	-46.79
Rice–wheat rotation	572.05	238.28	496.23	206.70	75.818	31.58
Rapeseed–maize rotation	133.92	151.40	248.46	280.90	-114.543	-129.50
Wheat–maize rotation	378.89	179.82	471.749	223.90	-92.859	-44.07

### 3.4. Analysis of Factors Influencing Potassium Balance in Farmland Soils

Table 4 presents the average balance values of soil potassium within a 500-m grid, as well as its relationships with the average values of associated influencing factors. The research area is divided grid-by-grid, with each grid serving as a sample point. Through correlation analysis of these sample points, we identified the correlation between soil potassium balance and various influencing factors, as shown in Table 4. Pearson's correlation analysis showed that all environmental factors except MAT showed significant or highly significant correlations with soil potassium balance (Table 4). Therefore, MAP, elevation, slope, population density, road density, and AK content were incorporated into the subsequent analysis.

**Table 4.** Pearson's correlation analyses among soil potassium balance and the various environmental factors.

	K Balance	MAT	MAP	Elevation	Slope	Aspect	Population Density	Road Density	AK
K balance	1	-0.002	-0.085 **	-0.062 **	-0.034 *	0.067 **	0.131 **	0.054 *	0.0144 **
MAT	-0.002	1	0.881 **	-0.853 **	-0.435 **	-0.017	0.162 **	-0.019	0.076 **
MAP	0.085 **	0.881 **	1	-0.734 **	-0.344 **	-0.023 *	0.107 **	-0.036	0.177 **
Elevation	-0.062 **	-0.853 **	-0.734 **	1	0.604 **	0.037 **	-0.189 **	-0.010	-0.030 **
Slope	-0.034 *	-0.435 **	-0.344 **	0.604 **	1	0.017	-0.123 **	-0.003	0.035 **
Aspect	0.067 **	-0.017	-0.023 *	0.037 **	0.017	1	-0.046 **	0.024	-0.017
Population density	0.131 **	0.162 **	0.107 **	-0.189 **	-0.123 **	-0.046 **	1	0.056 **	0.161 **
Road density	0.054 *	-0.019	-0.036	-0.010	-0.003	0.024	0.056 **	1	0.033
AK	-0.144 **	0.076 **	-0.177 **	-0.030 **	0.035 **	-0.017	0.161 **	0.033	1

Note: MAT means mean annual temperature; MAP means mean annual precipitation; AK means soil available potassium; \* and \*\* indicate t-test significant correlations at the 0.05 and 0.01 levels, respectively.

The slope direction and topographic factor variables were not significant, so they were excluded from the SEM model. The overall fit index of the final SEM model was  $\chi^2/\text{df} = 1.392$ , RMSEA = 0.009, and GFI = 1.000 (Figure 7), which satisfied the requirements for goodness of fit between the theoretical model and the data ( $\chi^2/\text{df} < 2$ , RMSEA < 0.1, GFI > 0.9), indicating that the constructed model was reliable. The contribution made by the environmental factors to the soil potassium balance was 20.8% (Figure 7). Specifically, the topographic factor had a direct positive effect of 0.243 on the potassium balance and indirect effects of -0.263, 0.063, and 0.011 for the anthropogenic activity factor, average annual precipitation, and soil AK content, respectively. Therefore, the total effect of the topographic factor on the potassium balance was 0.053. The anthropogenic activity factor had a direct positive effect of 0.559 on the potassium balance. Its indirect positive effect on

the potassium balance through its effects on soil AK was 0.238, leading to a total effect on the potassium balance of 0.797. However, MAP had a direct negative effect of  $-0.100$  on the potassium balance and an indirect negative effect of  $-0.029$  through its effect on soil AK content, resulting in a total effect of  $-0.129$  on the potassium balance. The soil AK had a direct positive effect of 0.408 on the potassium balance.

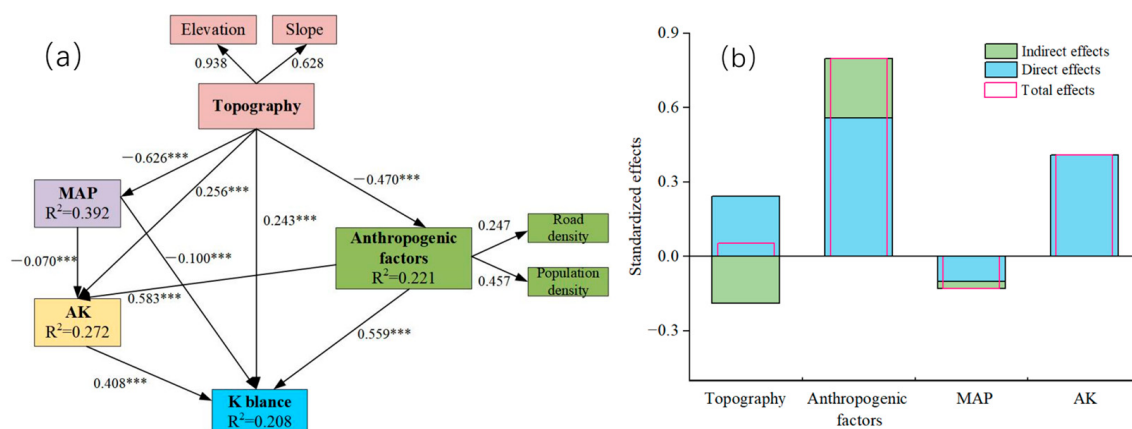


**Figure 7.** Structural equation model for K balance and the environmental factors. (a) Structural equation model for K balance and the environmental factors, (b) the standard effects of topography, anthropogenic factors, MAP and AK. Note: MAP means mean annual precipitation; AK means soil available potassium; \*\*\* indicates extremely significant effects ( $p < 0.001$ ).

#### 4. Discussion

In this study, both the NDVI and the MCARI were used to construct the decision-tree-based crop distribution extraction model. Rice and maize have different climatic characteristics, which means that they are well distinguished by the NDVI during their different growth periods [23]. Wheat and oilseed rape are similar to each other due to their growth cycles, which means that it is not appropriate to use the NDVI to distinguish between them. However, wheat and rape were separated by applying MCARI thresholds, which can discern significant differences between wheat and rape during their growth cycles [24]. The final extraction accuracies of the four crops, i.e., rice, maize, oilseed rape, and wheat, were more than 85%, indicating that the decision tree constructed in this study performed well [25]. The maize and wheat areas in the study area were much larger than the rice and oilseed rape areas, while the extracted crop rotation area was lower, which is probably due to local planting history, soil properties, and other factors [26].

The mean value for soil RAK in the study area was  $63.63 \text{ mg kg}^{-1}$  (Table 1), the mean soil RAK in the Yujiang hilly area of Jiangxi is  $74.00 \text{ mg kg}^{-1}$  [27], and the Pearl River Delta hilly area value is  $77.80 \text{ mg kg}^{-1}$  [28], which are all below the potassium deprivation threshold of  $80 \text{ mg kg}^{-1}$  [4]. This is mainly due to the long history of intensive cropping activity in the hilly areas of China. Crops such as maize, rape, and rice have high potassium demands for growth. However, potassium fertilizer inputs have been neglected for a long time in the areas in which these crops are grown, and this has led to the depletion of potassium reserves in the soil [9,29,30]. SAK, an important component of the soil AK reserve, is dynamically converted from partially slowly available to RAK when the soil is deficient in RAK [31]. However, soil SAK content in the study area was generally low or moderate, indicating the need for exogenous supplemental potassium inputs to meet crop-growth requirements. The spatial distribution of soil RAK in the study area showed that it was generally at a high level in the central townships and low in the northern and southern townships, suggesting that factors such as crop cultivation, field fertilization, and topography may have caused intra-regional differences in potassium content. SAK content was significantly high in central and east townships and low in the north and

south townships, mainly because its more stable nature is significantly influenced by natural factors.

In various crop rotation systems, significant differences exist in the sources of soil potassium, such as straw recycling, irrigation water, and rainfall input. Taking the rice–rapeseed rotation model as an example, all sources of potassium input are highest in this system, particularly straw recycling, which contributes up to  $57.91 \text{ kg K ha}^{-1} \text{ yr}^{-1}$ . This high input is likely attributable to the abundant organic matter provided by straw recycling, thereby elevating the potassium content in the soil [32]. Specific fertilizer management practices may have been adopted in the rice–rapeseed rotation model, as existing research demonstrates that appropriate use of potassium fertilizers can increase soil potassium levels [33]. Concurrently, soil types also influence potassium content and availability. For instance, clay soils usually retain potassium more effectively than sandy soils, which might lead to potassium leaching [34]. This study found that the most severe potassium deficiency occurred in the rapeseed–maize rotation model, while the deficiency was comparably mild in the rice–rapeseed and wheat–maize rotation models; only the rice–wheat rotation model showed a surplus of potassium. These variations are likely due to the differential demand and utilization efficiency of potassium among various crops and also depend on the stage of crop growth [35]. Lastly, compared to monoculture systems, crops in rotation systems generally exhibit higher demand for and utilization of potassium. In monoculture systems, crops usually have lower potassium uptake, resulting in a higher soil potassium balance. This, in turn, affects the overall soil potassium balance in the system [9,36].

In general, the higher the altitude, the lower the temperature, which is not conducive to the normal growth of crops such as maize, rape, and rice [37], and the greater the slope, the more severe the soil erosion and the greater the labor input required [38,39]. Thus, the high altitude and slope topographic factors lead to reduced cropping activity and decreased potassium export, whereas topography is significantly and positively correlated with potassium balance (Figure 7). In addition, topography is one of the determinants of soil water, nutrients, and temperature redistribution in certain regions [40,41]; therefore, it also has an indirect effect on potassium balance by affecting natural factors, such as MAP and soil AK content. For example, Liu et al. [42] showed that precipitation on the northeastern slope of the Tibetan Plateau was negatively related to altitude. Furthermore, sufficient precipitation can enhance crop productivity and thus potassium uptake [43], but it can also increase AK leaching loss from soil [3,44]; therefore, precipitation has a negative effect on soil AK content and potassium balance. Anthropogenic factors influence soil AK and potassium balance mainly through planting intensity and fertilizer management. On the one hand, the greater the road density, the more convenient the agricultural mechanization operation [45], while higher population density leads to greater food demand. Thus, high road and population densities increase crop planting intensity and aggravate potassium output. But, on the other hand, increased road density also promotes fertilizer management activity, and potassium fertilizer applications directly increase potassium inputs and the effective soil potassium content. Ultimately, the results from this study show that the combined effects of topography, precipitation, and anthropogenic factors led to soil AK content having a highly significant positive effect on potassium balance.

In the present study, topography, anthropogenic activities, precipitation, and soil effective potassium content explained 20.8% of the variation in potassium balance, but 79.2% remained unexplained. This unexplained portion may be related to differences in soil particle composition, basic chemical properties, and mineralogical characteristics. Soil particles are the basic structure of the soil porous medium and their composition is closely linked to the physical, chemical, and biological properties of soil. Previous studies have reported that fine particles (clay and powder) are the physical conservators of soil potassium and that the proportion of fine particles is an important factor controlling the variation of soil potassium content [46,47]. Zhuang et al. [48] pointed out that during seepage, fine particles migrate between large voids, leading to soil physical erosion, and the loss of potassium ions leads to chemical dissolution. Furthermore, soil particle composition

can also have an impact on crop growth [49]. For example, Huang et al. [50] showed that plant numbers and biomass were significantly greater in finer-grained soils. In addition, as important indicators of basic soil properties, adequate soil cation exchange, soil organic matter levels, and an appropriate pH not only ensure normal plant growth, but also influence soil potassium fixation and uptake capacity through ion exchange with  $\text{Al}^{3+}$ ,  $\text{Ca}^{2+}$ , and  $\text{Mg}^{2+}$  [51]. Similarly, clay minerals can be involved in potassium balance processes through ion exchange, dissolution release, and colloidal sorption [9,52,53], and the effects of different types of minerals on soil potassium are not uniform. For instance, 2:1 clay minerals are generally a reservoir of potassium in the soil, but are converted to vermiculite, chlorite, etc., when potassium becomes depleted [54]. Therefore, the above unexplained factors may have contributed to the fact that only 20.8% of variation in potassium balance was fully explained in the structural equation model, and should be explored in depth in future studies.

## 5. Conclusions

In this study, the spatial structure of the main crops within the study area was extracted using a decision tree algorithm based on multi-temporal Sentinel-2A imagery. The accuracy for crop extraction ranged from 84.65% to 89.36%, as compared to data from the Statistical Yearbook. The average amount of readily available potassium (RAK) in the soil was  $63.63 \text{ mg kg}^{-1}$ , while that of slowly available potassium (SAK) stood at  $649.77 \text{ mg kg}^{-1}$ . The spatial distribution patterns of both RAK and SAK in the soil predominantly exhibited high levels in the central townships and lower concentrations in the northern and southern townships. The soil potassium balance outcomes for various cropping patterns varied from  $-187.22$  to  $101.81 \text{ kg K ha}^{-1} \text{ yr}^{-1}$ , with the rape-maize rotation showing the most significant potassium deficit. Climate, topography, human activity, and soil AK together explained about 20% of the variation in soil potassium balance. Unexplained variations in the results are likely attributable to the omission of additional crops, such as vegetables and sweet potatoes. The differences in potassium input and output patterns for these unaccounted crops, as compared to the crops identified through remote sensing images, may have had some impact on the study results. Furthermore, the unexplained variation may also be attributed to the fact that the calculated potassium inputs and outputs were primarily derived from pertinent literature and field surveys, without taking into account the contribution of soil potassium supplementation through organic fertilizers, such as livestock and poultry manure. Hence, future studies should aim to acquire more precise data regarding regional cropping patterns and the specific parameters employed in potassium balance calculations. This would help to better elucidate the factors affecting soil potassium balance and establish a solid theoretical foundation for the precise management of soil potassium fertility.

**Author Contributions:** Conceptualization, S.W. and T.L.; Methodology, S.W. and P.P.; Data Collection, Z.L.; Analysis and Interpretation of Results, L.L. and G.W.; Visualization, Y.X.; Draft Manuscript Preparation, S.W.; Funding Acquisition, Q.L.; S.W. and Z.L. contributed equally to this work and should be considered co-first authors. All authors have read and agreed to the published version of the manuscript.

**Funding:** This research was funded by the strategic priority research program of the Chinese Academy of Sciences (grant number: XDA23090501).

**Institutional Review Board Statement:** Not applicable.

**Informed Consent Statement:** Not applicable.

**Data Availability Statement:** No new data has been created.

**Conflicts of Interest:** The authors declare no conflict of interest.

## References

1. Soumare, A.; Sarr, D.; Diedhiou, A.G. Potassium sources, microorganisms and plant nutrition: Challenges and future research directions. *Pedosphere* **2023**, *33*, 105–115. [[CrossRef](#)]
2. Zörb, C.; Senbayram, M.; Peiter, E. Potassium in agriculture—Status and perspectives. *J. Plant Physiol.* **2014**, *171*, 656–669. [[CrossRef](#)] [[PubMed](#)]
3. Li, T.; Liang, J.; Chen, X.; Wang, H.; Zhang, S.; Pu, Y.; Xu, X.; Li, H.; Xu, J.; Wu, X.; et al. The interacting roles and relative importance of climate, topography, soil properties and mineralogical composition on soil potassium variations at a national scale in China. *Catena* **2021**, *196*, 104875. [[CrossRef](#)]
4. He, P.; Yang, L.; Xu, X.; Zhao, S.; Chen, F.; Li, S.; Tu, S.; Jin, J.; Johnston, A.M. Temporal and spatial variation of soil available potassium in China (1990–2012). *Field Crop. Res.* **2015**, *173*, 49–56. [[CrossRef](#)]
5. Liu, F.; Wu, H.; Zhao, Y.; Li, D.; Yang, J.; Song, X.; Shi, Z.; Zhu, A.; Zhang, G. Mapping high resolution National Soil Information Grids of China. *Sci. Bull.* **2022**, *67*, 328–340. [[CrossRef](#)] [[PubMed](#)]
6. Li, T.; Wang, H.; Wang, J.; Zhou, Z.; Zhou, J. Exploring the potential of phyllosilicate minerals as potassium fertilizers using sodium tetraphenylboron and intensive cropping with perennial ryegrass. *Sci. Rep.* **2015**, *5*, 9249. [[CrossRef](#)] [[PubMed](#)]
7. Xi, S.; Chu, H.; Zhou, Z.; Li, T.; Zhang, S.; Xu, X.; Pu, Y.; Wang, G.; Jia, Y.; Liu, X. Effect of potassium fertilizer on tea yield and quality: A meta-analysis. *Eur. J. Agron.* **2023**, *144*, 126767. [[CrossRef](#)]
8. Yadav, S.K.; Benbi, D.K.; Toor, A.S. Effect of long-term application of rice straw, farmyard manure and inorganic fertilizer on potassium dynamics in soil. *Arch. Agron. Soil Sci.* **2019**, *65*, 374–384. [[CrossRef](#)]
9. Das, D.; Sahoo, J.; Raza, M.B.; Barman, M.; Das, R. Ongoing soil potassium depletion under intensive cropping in India and probable mitigation strategies. A review. *Agron. Sustain. Dev.* **2022**, *42*, 4. [[CrossRef](#)]
10. Nguyen, T.T.; Sasaki, Y.; Aizawa, M.; Kakuda, K.; Fujii, H. Potassium balance in paddy fields under conventional rice straw recycling versus cow dung compost application in mixed crop–livestock systems in Japan. *Soil Sci. Plant Nutr.* **2023**, *69*, 36–44. [[CrossRef](#)]
11. Oenema, O.; Kros, H.; de Vries, W. Approaches and uncertainties in nutrient budgets: Implications for nutrient management and environmental policies. *Eur. J. Agron.* **2003**, *20*, 3–16. [[CrossRef](#)]
12. Li, Y.; Xia, G.; Wu, Q.; Chen, W.; Lin, W.; Zhang, Z.; Chen, Y.; Chen, T.; Siddique, K.H.M.; Chi, D. Zeolite increases grain yield and potassium balance in paddy fields. *Geoderma* **2022**, *405*, 115397. [[CrossRef](#)]
13. Zhang, Z.; Liu, D.; Wu, M.; Xia, Y.; Zhang, F.; Fan, X. Long-term straw returning improve soil K balance and potassium supplying ability under rice and wheat cultivation. *Sci. Rep.* **2021**, *11*, 22260. [[CrossRef](#)] [[PubMed](#)]
14. Linquist, B.A.; Campbell, J.C.; Southard, R.J. Assessment of potassium soil balances and availability in high yielding rice systems. *Nutr. Cycl. Agroecol.* **2022**, *122*, 255–271. [[CrossRef](#)]
15. Liu, Y.; Ma, J.; Ding, W.; He, W.; Lei, Q.; Gao, Q.; He, P. Temporal and spatial variation of potassium balance in agri-cultural land at national and regional levels in China. *PLoS ONE* **2017**, *12*, e184156.
16. Lu, R. *Methods of Soil and Geochemistry Analysis*; China Agricultural Science and Technology Press: Beijing, China, 2000; pp. 62–141.
17. Gao, Z.; Guo, D.; Ryu, D.; Western, A.W. Training sample selection for robust multi-year within-season crop classification using machine learning. *Comput. Electron. Agric.* **2023**, *210*, 107927. [[CrossRef](#)]
18. Xia, Y.; Liu, D.; Zhang, F.; Xiong, G.; Duan, X.; Wu, M.; Fan, X. Potassium balance in the agroecosystem of the main cropping systems in Hubei Province. *Chin. J. Ecol.* **2014**, *33*, 2395–2401. [[CrossRef](#)]
19. Li, S.; Jin, J. Characteristics of Nutrient Input/Output and Nutrient Balance in Different Regions of China. *Sci. Agric. Sin.* **2011**, *44*, 4207–4229.
20. He, X. Current Situation and Countermeasures of Comprehensive Utilization of Crop Straw in Suining City. *Mod. Agric. Sci. Technol.* **2018**, *179*–180.
21. Liu, X. Study on Nutrients Balance and Requirement in Agriculture Production in China. Ph.D. Thesis, Chinese Academy of Agricultural Sciences, Beijing, China, 2018.
22. West, S.G.; Taylor, A.B.; Wu, W. Model Fit and Model Selection in Structural Equation Modeling. In *Handbook of Structural Equation Modeling*; The Guilford Press: New York, NY, USA, 2012; pp. 209–231.
23. Li, X.; Jiang, Q. Extraction of farmland classification based on multi-temporal remote sensing data. *Nongye Gongcheng Xuebao/Trans. Chin. Soc. Agric. Eng.* **2015**, *31*, 145–150.
24. Mercier, A.; Betbeder, J.; Baudry, J.; Le Roux, V.; Spicher, F.; Lacoux, J.; Roger, D.; Hubert-Moy, L. Evaluation of Sentinel-1 & 2 time series for predicting wheat and rapeseed phenological stages. *ISPRS J. Photogramm.* **2020**, *163*, 231–256. [[CrossRef](#)]
25. Hafeez, M.A.; Rashid, M.; Tariq, H.; Abideen, Z.U.; Alotaibi, S.S.; Sinky, M.H. Performance Improvement of Decision Tree: A Robust Classifier Using Tabu Search Algorithm. *Appl. Sci.* **2021**, *11*, 6728. [[CrossRef](#)]
26. Liu, J.; Yang, K.; Tariq, A.; Lu, L.; Soufan, W.; El Sabagh, A. Interaction of climate, topography and soil properties with cropland and cropping pattern using remote sensing data and machine learning methods. *Egypt. J. Remote Sens. Space Sci.* **2023**, *26*, 415–426. [[CrossRef](#)]

27. Li, P.; Zhang, T.; Wang, X.; Yu, D. Development of biological soil quality indicator system for subtropical China. *Soil Tillage Res.* **2013**, *126*, 112–118. [[CrossRef](#)]
28. Wang, R.; Zou, R.; Liu, J.; Liu, L.; Hu, Y. Spatial Distribution of Soil Nutrients in Farmland in a Hilly Region of the Pearl River Delta in China Based on Geostatistics and the Inverse Distance Weighting Method. *Agriculture* **2021**, *11*, 50. [[CrossRef](#)]
29. Ren, T.; Lu, J.; Li, H.; Zou, J.; Xu, H.; Liu, X.; Li, X. Potassium-fertilizer management in winter oilseed-rape production in China. *J. Plant Nutr. Soil Sc.* **2013**, *176*, 429–440. [[CrossRef](#)]
30. Zhao, X.; Gao, S.; Lu, D.; Wang, H.; Chen, X.; Zhou, J.; Zhang, L. Can Potassium Silicate Mineral Products Replace Conventional Potassium Fertilizers in Rice–Wheat Rotation? *Agron. J.* **2019**, *111*, 2075–2083. [[CrossRef](#)]
31. WANG, H.; CHENG, W.; LI, T.; ZHOU, J.; CHEN, X. Can Nonexchangeable Potassium be Differentiated from Structural Potassium in Soils? *Pedosphere* **2016**, *26*, 206–215. [[CrossRef](#)]
32. Han, Y.; Ma, W.; Zhou, B.; Salah, A.; Geng, M.; Cao, C.; Zhan, M.; Zhao, M. Straw Return Increases Crop Grain Yields and K-Use Efficiency under a Maize–Rice Cropping System. *Crop J.* **2021**, *9*, 168–180. [[CrossRef](#)]
33. Li, J.; Gan, G.; Chen, X.; Zou, J. Effects of Long-Term Straw Management and Potassium Fertilization on Crop Yield, Soil Properties, and Microbial Community in a Rice–Oilseed Rape Rotation. *Agriculture* **2021**, *11*, 1233. [[CrossRef](#)]
34. Hamoud, Y.A.; Wang, Z.; Guo, X.; Shaghaleh, H.; Sheteiwly, M.; Chen, S.; Qiu, R.; Elbashier, M.M.A. Effect of Irrigation Regimes and Soil Texture on the Potassium Utilization Efficiency of Rice. *Agronomy* **2019**, *9*, 100. [[CrossRef](#)]
35. Singh, V.K.; Dwivedi, B.S.; Rathore, S.S.; Mishra, R.P.; Satyanarayana, T.; Majumdar, K. Timing Potassium Applications to Synchronize with Plant Demand. In *Improving Potassium Recommendations for Agricultural Crops*; Murrell, T.S., Mikkelsen, R.L., Sulewski, G., Norton, R., Thompson, M.L., Eds.; Springer International Publishing: Cham, Switzerland, 2021; pp. 363–384. [[CrossRef](#)]
36. Steiner, F.; Pivetta, L.A.; Castoldi, G.; Costa, M.S.S.d.M.; Costa, L.A.d.M. Phosphorus and Potassium Balance in Soil under Crop Rotation and Fertilization. *Semin. Ciênc. Agrár.* **2012**, *33*, 2173–2186. [[CrossRef](#)]
37. Oteros, J.; García-Mozo, H.; Vázquez, L.; Mestre, A.; Domínguez-Vilches, E.; Galán, C. Modelling olive phenological response to weather and topography. *Agric. Ecosyst. Environ.* **2013**, *179*, 62–68. [[CrossRef](#)]
38. Wei, W.; Chen, L.; Zhang, H.; Yang, L.; Yu, Y.; Chen, J. Effects of crop rotation and rainfall on water erosion on a gentle slope in the hilly loess area, China. *Catena* **2014**, *123*, 205–214. [[CrossRef](#)]
39. Tang, Y.; Lu, X.; Yi, J.; Wang, H.; Zhang, X.; Zheng, W. Evaluating the spatial spillover effect of farmland use transition on grain production—An empirical study in Hubei Province, China. *Ecol. Indic.* **2021**, *125*, 107478. [[CrossRef](#)]
40. Lin, Y.; Prentice, S.E.; Tran, T.; Bingham, N.L.; King, J.Y.; Chadwick, O.A. Modeling deep soil properties on California grassland hillslopes using LiDAR digital elevation models. *Geoderma Reg.* **2016**, *7*, 67–75. [[CrossRef](#)]
41. Dalzell, B.J.; Fissore, C.; Nater, E.A. Topography and land use impact erosion and soil organic carbon burial over decadal timescales. *Catena* **2022**, *218*, 106578. [[CrossRef](#)]
42. Liu, W.; Zhang, Q.; Fu, Z.; Chen, X.; Li, H. Analysis and Estimation of Geographical and Topographic Influencing Factors for Precipitation Distribution over Complex Terrains: A Case of the Northeast Slope of the Qinghai–Tibet Plateau. *Atmosphere* **2018**, *9*, 349. [[CrossRef](#)]
43. Wang, Y.; Shen, Y.; Xie, Y.; Ma, H.; Li, W.; Luo, X.; Zhang, H.; Zhang, Y.; Li, J. Changes in precipitation have both direct and indirect effects on typical steppe aboveground net primary productivity in Loess Plateau, China. *Plant Soil* **2023**, *484*, 503–515. [[CrossRef](#)]
44. Cappuccio, F.P.; Buchanan, L.A.; Ji, C.; Siani, A.; Miller, M.A. Systematic review and meta-analysis of randomised controlled trials on the effects of potassium supplements on serum potassium and creatinine. *BMJ Open* **2016**, *6*, e11716. [[CrossRef](#)]
45. Mottaleb, K.A.; Krupnik, T.J.; Erenstein, O. Factors associated with small-scale agricultural machinery adoption in Bangladesh: Census findings. *J. Rural Stud.* **2016**, *46*, 155–168. [[CrossRef](#)] [[PubMed](#)]
46. Ajiboye, A.G.; Ogunwale, A.J. Forms and distribution of potassium in particle size fractions on talc overburden soils in Nigeria. *Arch. Agron. Soil Sci.* **2013**, *59*, 247–258. [[CrossRef](#)]
47. Chen, Y.; Huang, L.; Cheng, L.; Liu, Z.; Bin, X. Straw returning and potassium fertilization affect clay mineralogy and available potassium. *Nutr. Cycl. Agroecosy.* **2023**, *126*, 195–211. [[CrossRef](#)]
48. Zhuang, J.; Peng, J.; Zhu, Y.; Leng, Y.; Zhu, X.; Huang, W. The internal erosion process and effects of undisturbed loess due to water infiltration. *Landslides* **2021**, *18*, 629–638. [[CrossRef](#)]
49. Zygalakis, K.C.; Kirk, G.J.D.; Jones, D.L.; Wissuwa, M.; Roose, T. A dual porosity model of nutrient uptake by root hairs. *N. Phytol.* **2011**, *192*, 676–688. [[CrossRef](#)]
50. Huang, L.; Dong, B.; Xue, W.; Peng, Y.; Zhang, M.; Yu, F. Soil Particle Heterogeneity Affects the Growth of a Rhizoma-tous Wetland Plant. *PLoS ONE* **2013**, *8*, e69836.
51. Golestanifard, A.; Santner, J.; Aryan, A.; Kaul, H.; Wenzel, W.W. Potassium fixation in northern Iranian paddy soils. *Geoderma* **2020**, *375*, 114475. [[CrossRef](#)]
52. Portela, E.; Monteiro, F.; Fonseca, M.; Abreu, M.M. Effect of soil mineralogy on potassium fixation in soils developed on different parent material. *Geoderma* **2019**, *343*, 226–234. [[CrossRef](#)]

53. Simonsson, M.; Hillier, S.; Öborn, I. Changes in clay minerals and potassium fixation capacity as a result of release and fixation of potassium in long-term field experiments. *Geoderma* **2009**, *151*, 109–120. [[CrossRef](#)]
54. Barré, P.; Velde, B.; Fontaine, C.; Catel, N.; Abbadie, L. Which 2:1 clay minerals are involved in the soil potassium reservoir? Insights from potassium addition or removal experiments on three temperate grassland soil clay assemblages. *Geoderma* **2008**, *146*, 216–223. [[CrossRef](#)]

**Disclaimer/Publisher’s Note:** The statements, opinions and data contained in all publications are solely those of the individual author(s) and contributor(s) and not of MDPI and/or the editor(s). MDPI and/or the editor(s) disclaim responsibility for any injury to people or property resulting from any ideas, methods, instructions or products referred to in the content.